Electronic Supplementary Material (ESI) for Journal of Materials Chemistry A.

Supporting Information

Boosting the performance of lithium metal capacitor with a Li composite anode

Bao Liu[1,2], Jiangtao Chen[1], Bingjun Yang[1,2], Lingyang Liu [1,2], Yinglun Sun[1,2], Ruilin Hou[1,2], Zifeng Lin[3], Xingbin Yan[1,2]*

B. Liu, J.T. Chen, B. J. Yang, L. Y. Liu, Y. L. Sun, R. L. Hou, Prof. X. B. Yan
Laboratory of Clean Energy Chemistry and Materials, State Key Laboratory of Solid Lubrication, Lanzhou Institute of Chemical Physics, Chinese Academy of Sciences, Lanzhou 730000, P. R. China.

Center of Materials Science and Optoelectronics Engineering, University of Chinese Academy of Sciences, Beijing 100049, P. R. China
E-mail: xbyan@licp.cas.cn (X. B. Yan)

Prof. Z. F. Lin
College of Materials Science and Engineering, Sichuan University, Chengdu 610065, P. R. China

Prof. Z. H. Zeng
Davidson School of Chemical Engineering, Purdue University, West Lafayette, IN 47907 United States

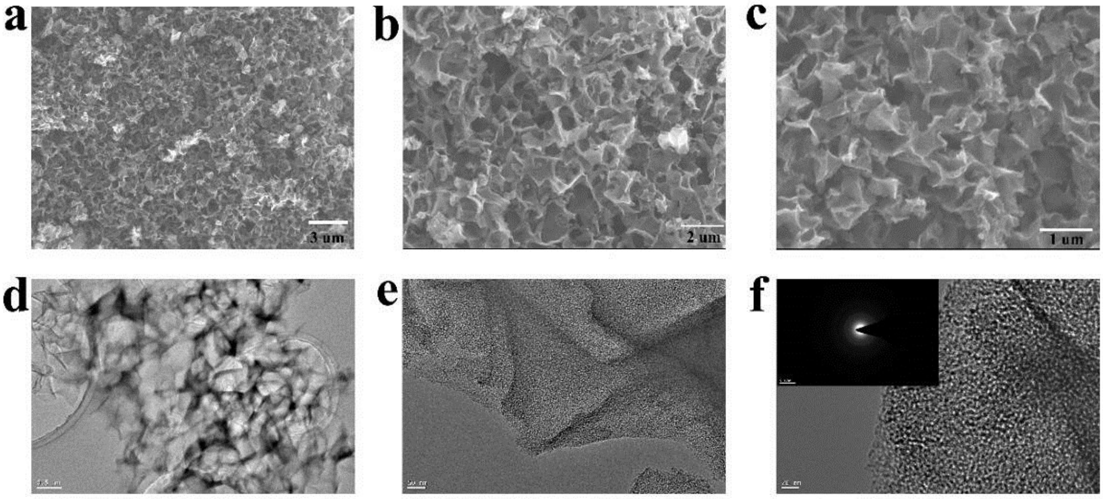

Fig. S1. Morphology of 3D-SAC. **(a-c)** SEM images at different magnifications. (**d-f)** TEM images at different magnifications, and the inset in **(f)** is the selected electron diffraction pattern.

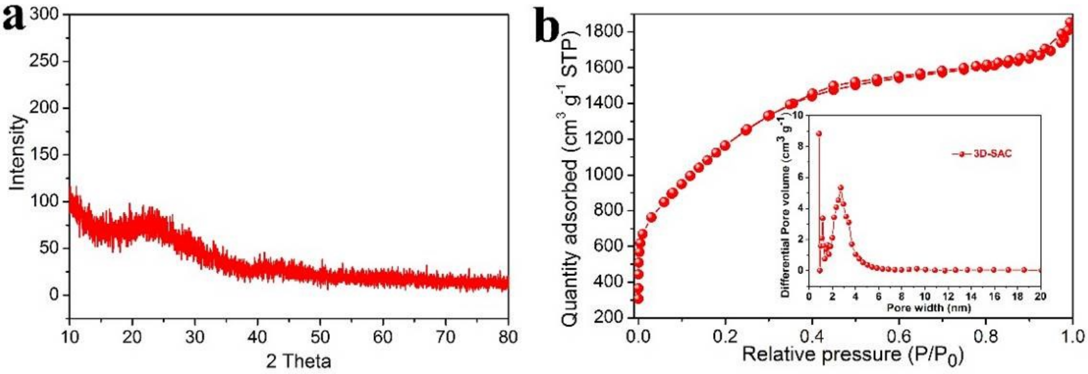

Fig. S2. XRD and the porous properties of 3D-SAC. **(a)** XRD pattern. (**b**) Nitrogen adsorption/desorption isotherm curve and the corresponding pore size distribution (inset).

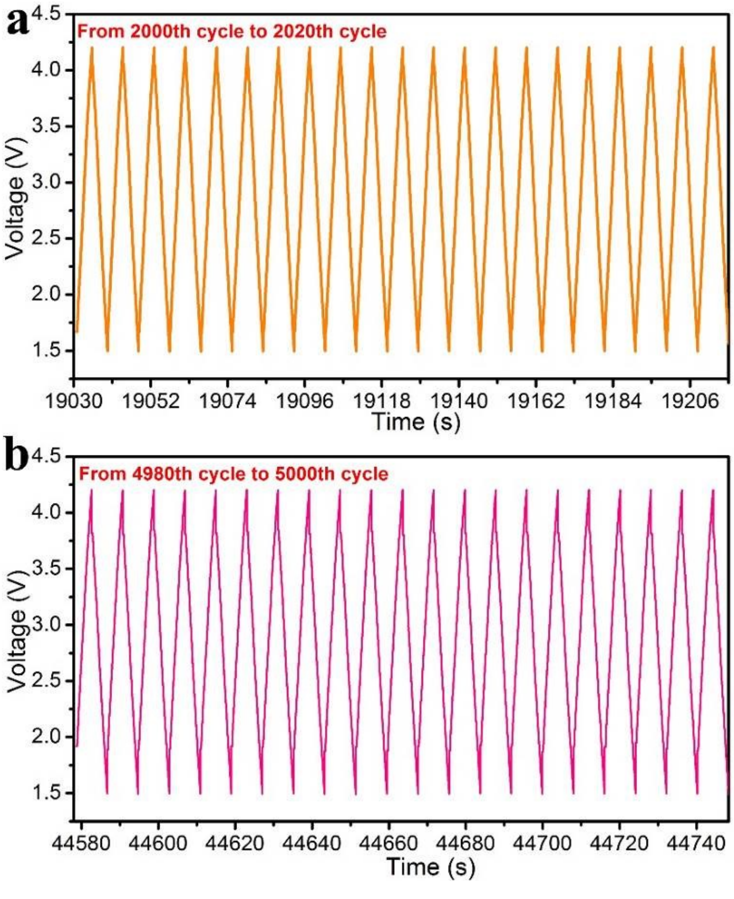

Fig. S3. Voltage curves of LMC at 2 A g^{-1} in the voltage window of 1.5-4.3 V. **(a)** Continuous charge-discharge curves from the 2000th to 2020th. (**b**) Continuous charge-discharge curves from the 4980th to 5000th.

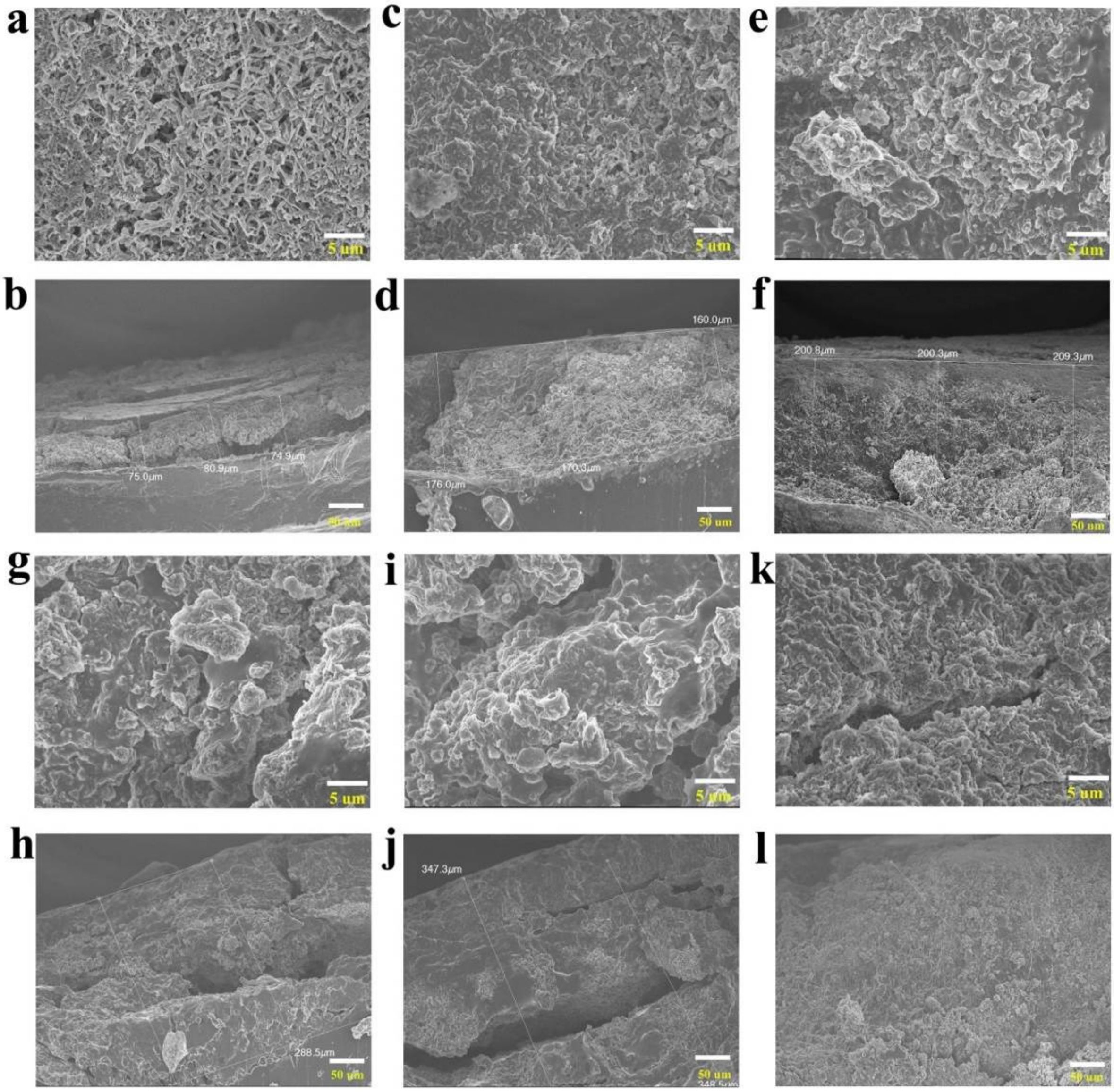

Fig. S4. Top-view and cross-section SEM images of Li anode after different cycles. (**a**, **b**) after 100 cycles. (**c**, **d**) after 1000 cycles. (**e**, **f**) after 2000 cycles. (**g**, **h**) after 3000 cycles. (**i**, **j**) after 4000 cycles. (**k**, **l**) after 5000 cycles.

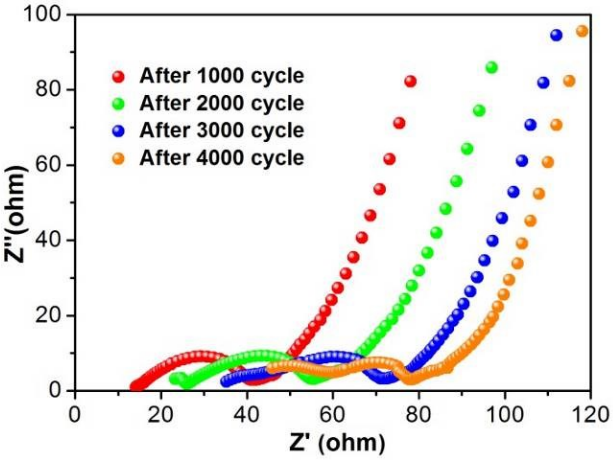

Fig. S5. Impedance plots of LMC after 1000, 2000, 3000 and 4000 cycles.

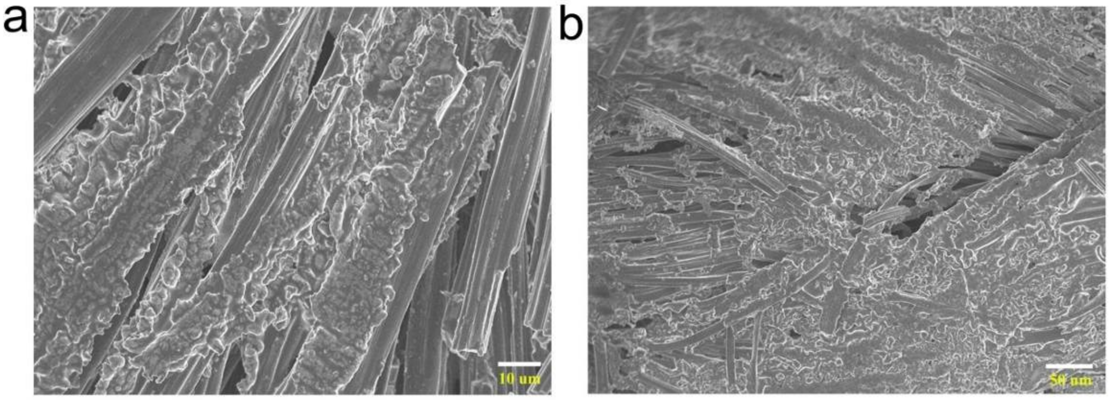

Fig. S6. SEM images of deposited Li on the backside of Au@CCS with a plating capacity of 2.0 mAh cm^{-2}, demonstrating the dendrite-free Li deposition on this substrate.

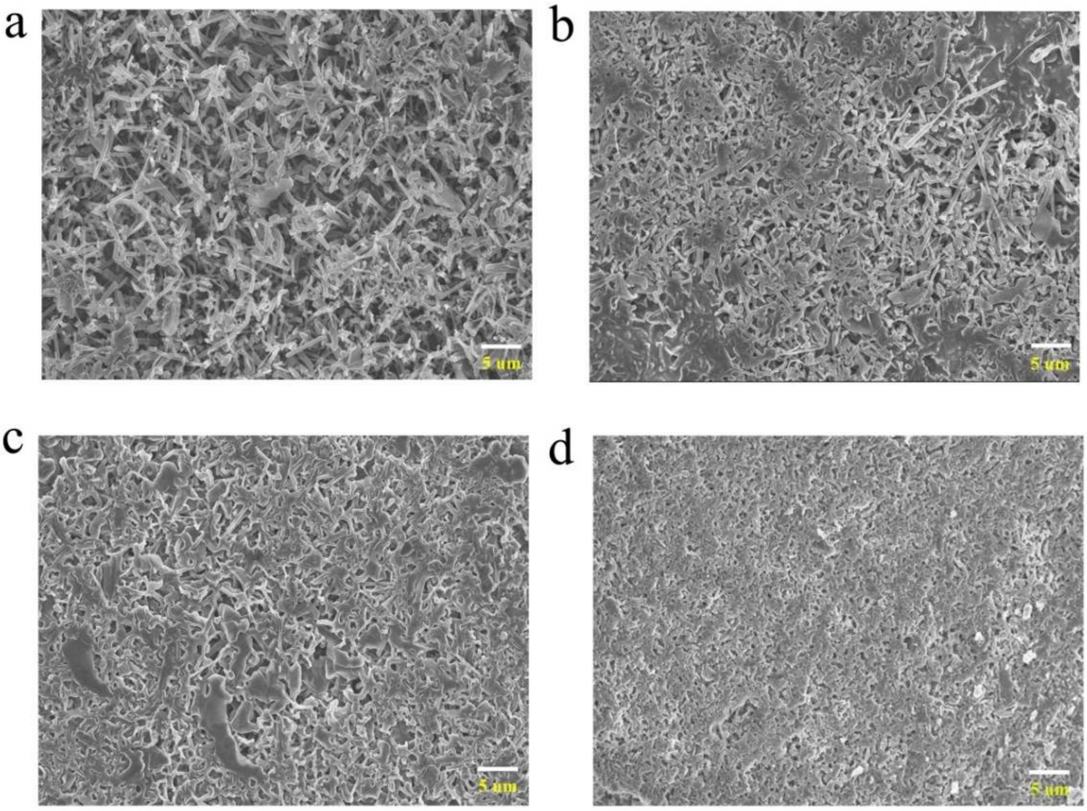

Fig. S7. SEM images of deposited Li on Cu foil current collector with plating capacity of (**a)** 0.5 mAh cm^{-2}, (**b)** 1.0 mAh cm^{-2} and (**c**) 2.0 mAh cm^{-2}, and (**d)** SEM image of the cycled Cu foil after 50 cycles of plating/stripping at a current density of 2.0 mA cm^{-2} and a capacity of 2.0 mAh cm^{-2}.

It was observed that wire-shaped Li deposits were formed on the surface of Cu current collector, regardless of plating capacity (Supplementary Fig. ~~S22a~~S7a-c), and the Li deposits would evolve into brittle, thick and porous "dead Li" with the repeated Li plating and stripping (Supplementary Fig. ~~S22d~~S7d).

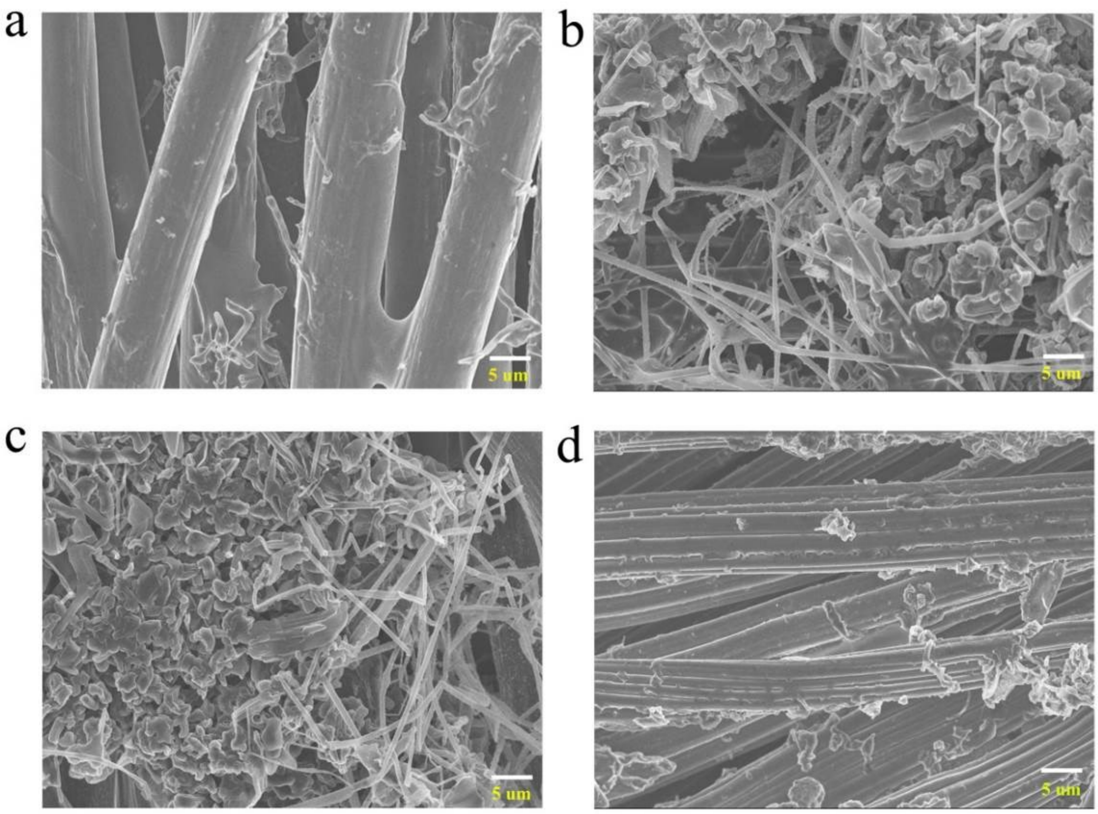

Fig. S8. SEM images of electrochemically deposited Li on carbon cloth current collector with plating capacity of (**a)** 0.5 mAh cm^{-2}, (**b)** 1.0 mAh cm^{-2}, (**c**) 2.0 mAh cm^{-2} and (**d)** SEM image of the cycled carbon cloth after 50 cycles of plating/stripping at a current density of 2.0 mA cm^{-2} and a capacity of 2.0 mAh cm^{-2}.

Though the carbon fibers matrix has the porous structure and conductive network for Li deposition, the dendritic Li blocks randomly distributed on the surface and filled in the gaps of carbon fibers with a plating capacity of 0.5 mAh cm^{-2} (Supplementary Fig. ~~S23a~~S8a). These blocks gradually involved into mossy Li deposits with the further increase of Li plating capacity (Supplementary Fig. ~~S23b~~S8b-c). After 50 cycles, massive and messy Li dendrites were dispersed on the surface of carbon cloth (Supplementary Fig. ~~S23d~~S8d).

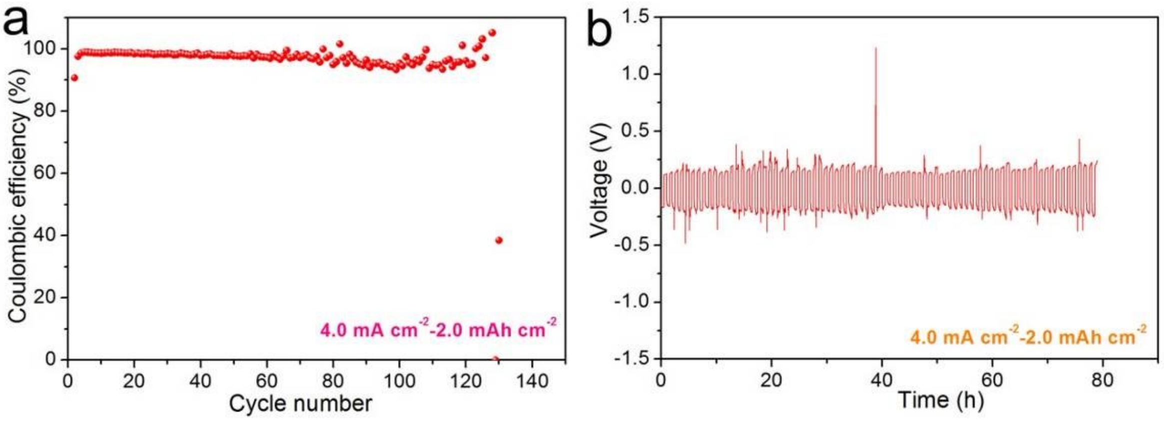

Fig. S9. (a) CEs of Au@CCS cathode cycled at 4.0 mA cm^{-2} with a cycling capacity of 2.0 mAh cm^{-2}. **(b)** Cycling performance of Li//Li-Au@CCS symmetric cell at 4.0 mA cm^{-2} with a fixed capacity of 2.0 mAh cm^{-2}.

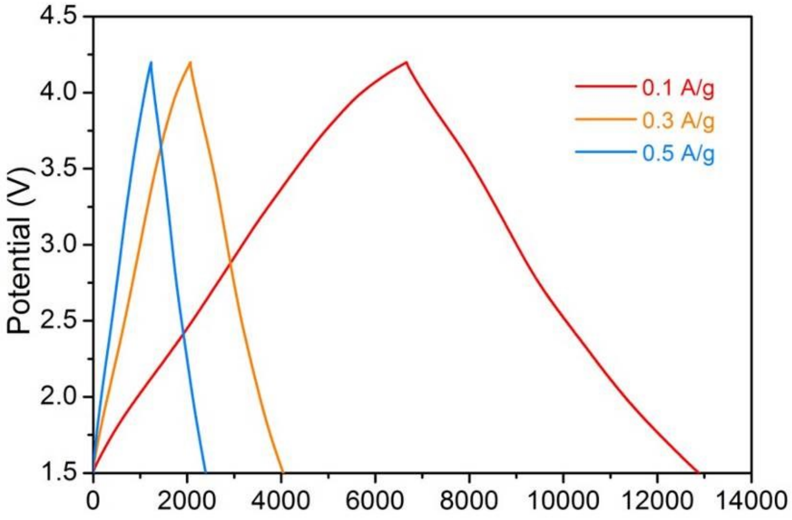

Fig. S10. GCD profiles of LMC paring with Li-Au@CCS anode at different current rates in the working voltage window of 1.5-4.2 V.

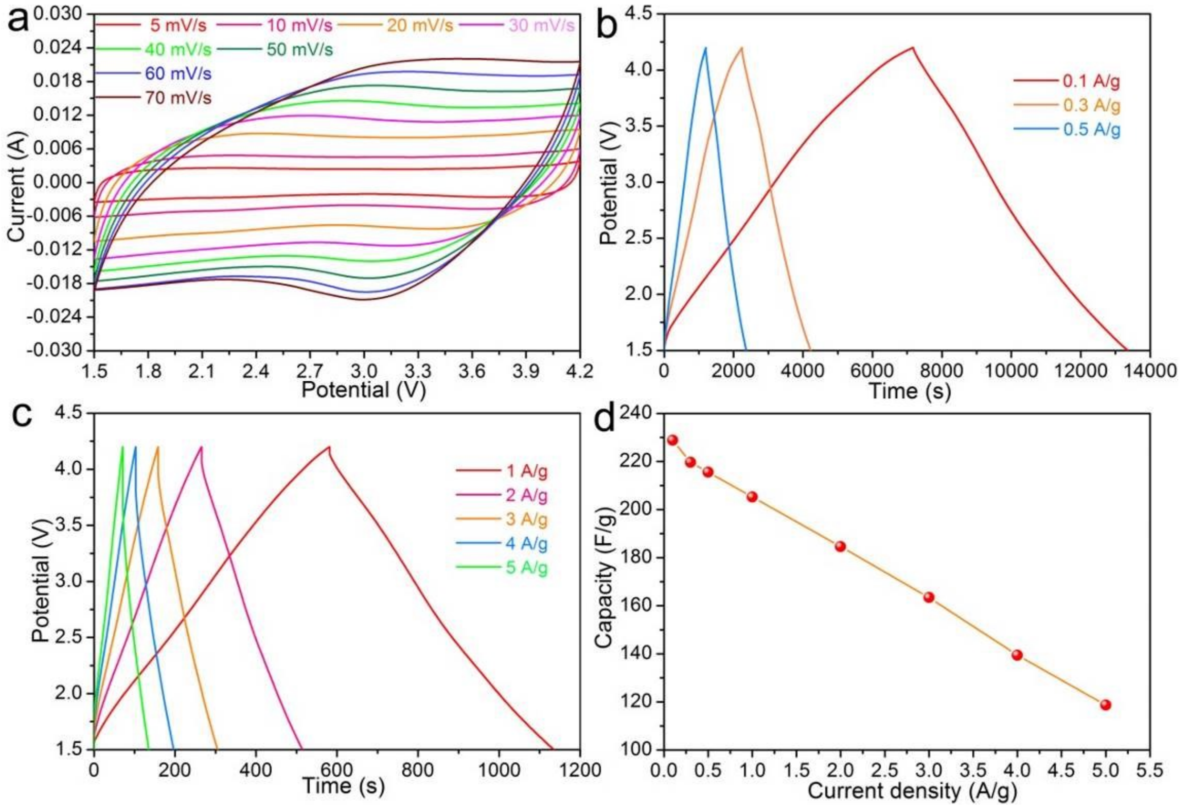

Fig. S11. Electrochemical performance of LMC paring with Li-Cu anode. (**a**) CV profiles at different scan rates in the working voltage window of 1.5-4.2 V. (**b** and **c**) GCD profiles at different current rates in the working voltage window of 1.5-4.2V. (**d**) Specific capacitances at different current rates.

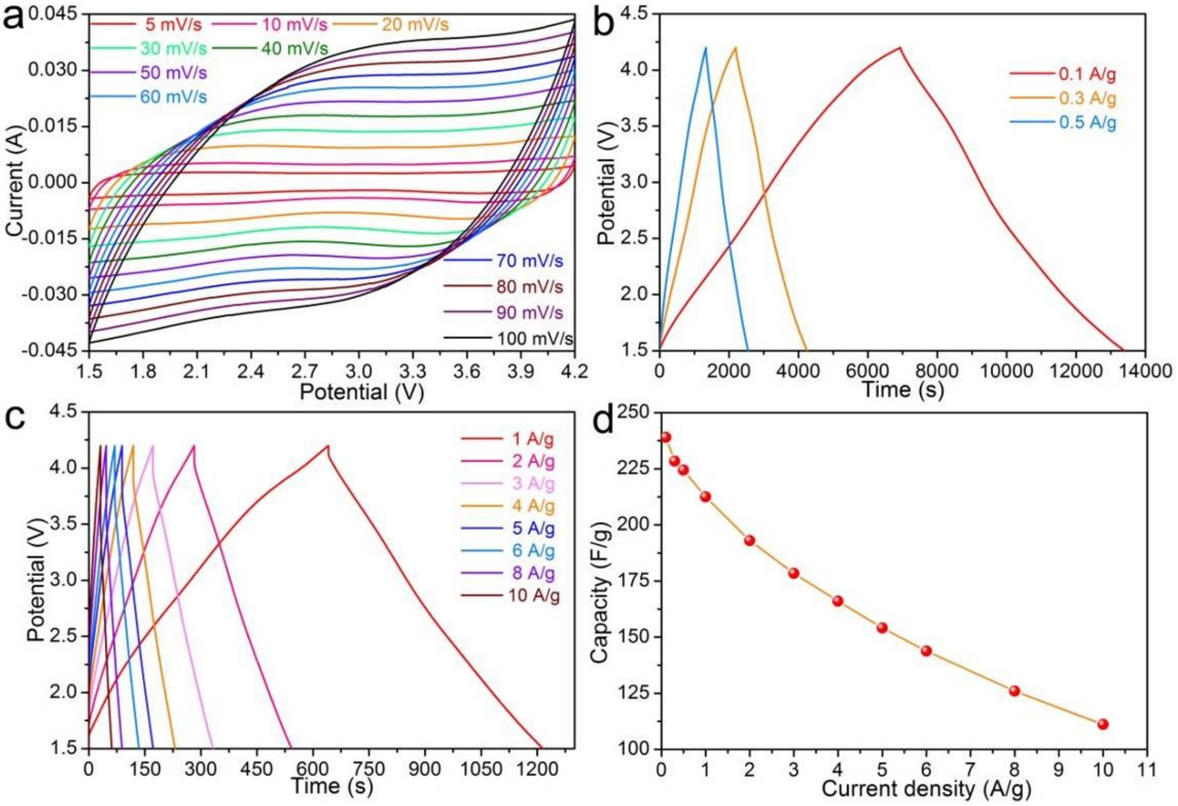

Fig. S12. Electrochemical performance of LMC paring with Li-CCS anode. (**a)** CV profiles at different scan rates in the working voltage window of 1.5-4.2 V. (**b** and **c**) GCD profiles at different current rates in the working voltage window of 1.5-4.2 V. (**d**) Specific capacitances at different current rates.

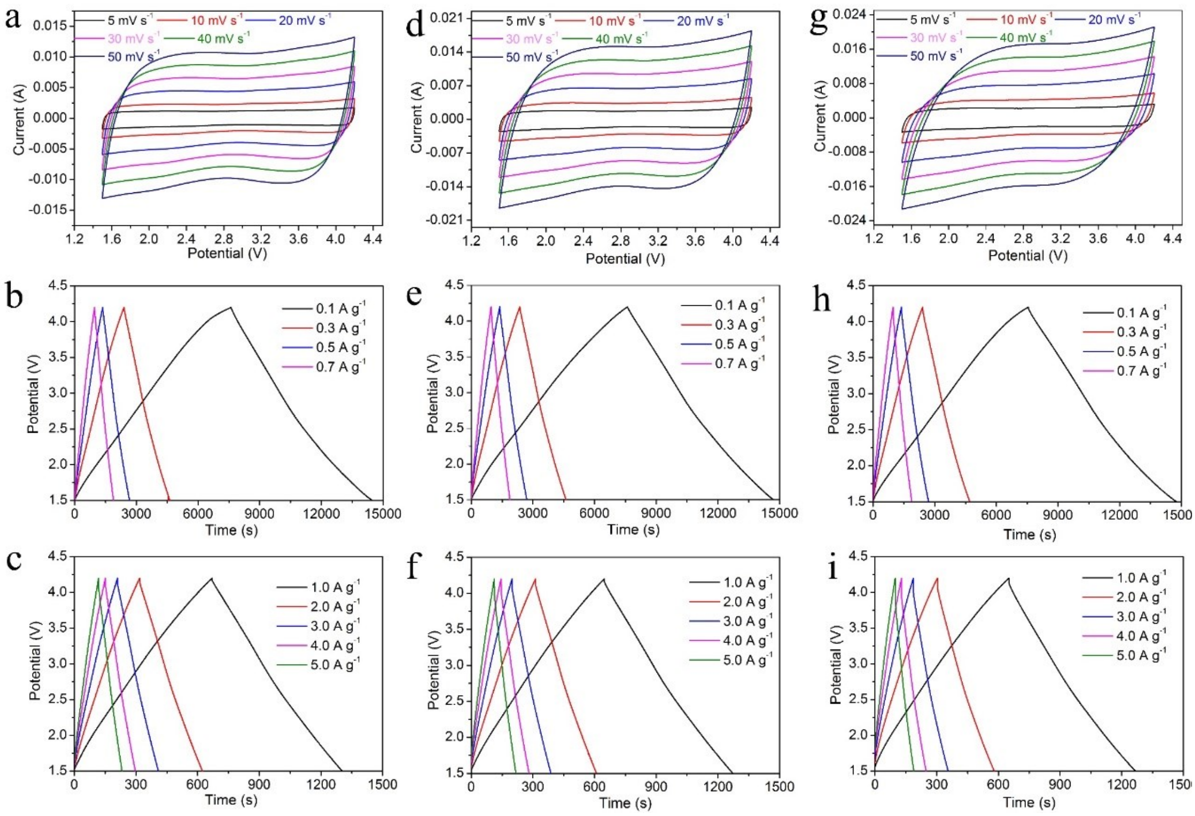

Fig. S13. Electrochemical performance of LMCs paring with Li-CCS anodes and 3D-SAC cathodes with different cathode loadings in the working voltage window of 1.5-4.2 V. (**a-c**) CV and GCD profiles of LMC with a cathode loading of 0.9 mg cm^{-2}. (**d-f**) CV and GCD profiles of LMC with a cathode loading of 1.3 mg cm^{-2}. (**g-i**) CV and GCD profiles of LMC with a cathode loading of 1.8 mg cm^{-2}. The current densities used for GCD measurement were based on the mass of 3D-SAC cathode.

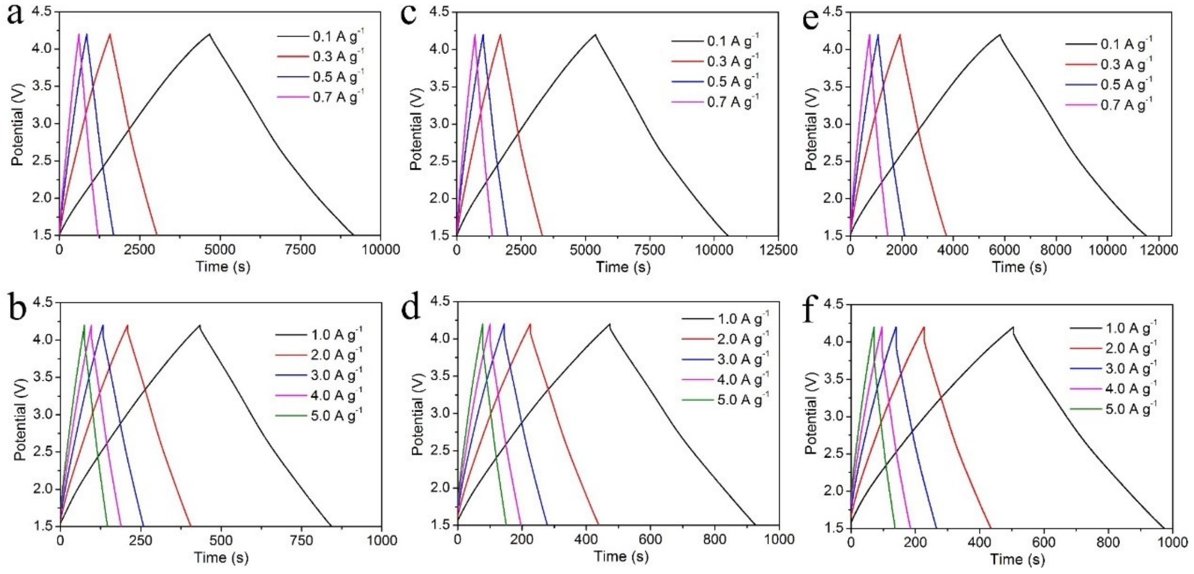

Fig. S14. Electrochemical performance of LMCs paring with Li-CCS anodes and 3D-SAC cathodes with different cathode loadings in the working voltage window of 1.5-4.2 V. (**a-b**) GCD profiles of

LMC with a cathode loading of 0.9 mg cm^{-2}. (**c-d**) GCD profiles of LMC with a cathode loading of 1.3 mg cm^{-2}. (**e-f**) GCD profiles of LMC with a cathode loading of 1.8 mg cm^{-2}. The current densities used for GCD measurement were based on the total mass of both 3D-SAC cathode and Li metal anode.

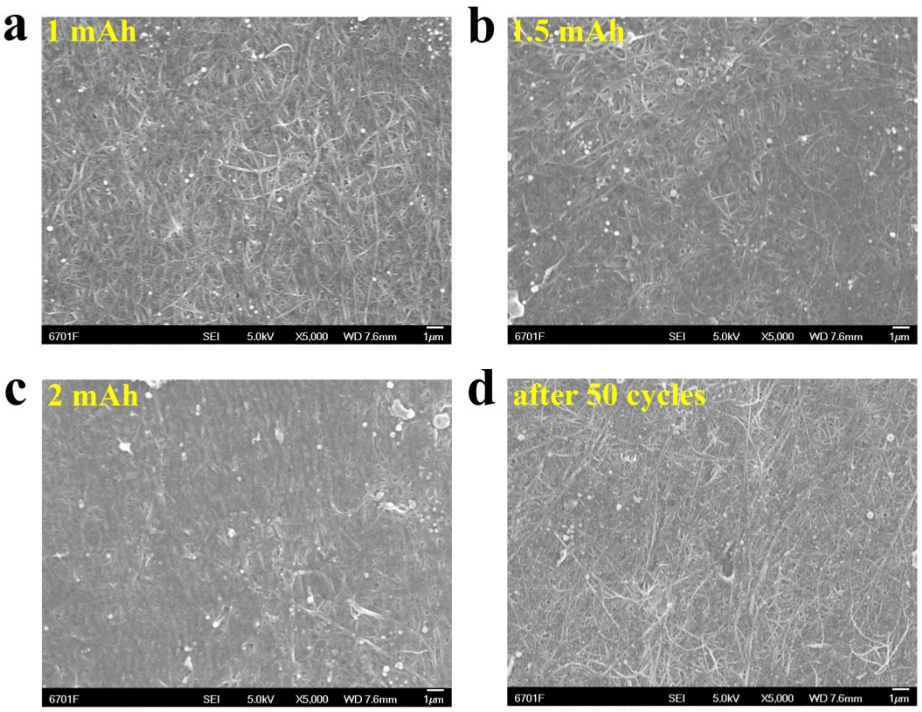

Fig. S15. The morphology characterization of Li-CNT composite anode. SEM images of electrochemically deposited Li on CNT film current collector with plating capacity of (**a**) 1.0 mAh cm^{-2}, (**b**) 1.5 mAh cm^{-2}, (**c**) 2.0 mAh cm^{-2} and (**d**) SEM image of the cycled Li-CNT composite anode after 50 cycles of plating/stripping at a current density of 1.0 mA cm^{-2} and a capacity of 1.0 mAh cm^{-2}.

Table S1 Comparison of the electrochemical performance of LMC with state-of-the-art LICs and LMBs.

Anodes/ Cathodes	**Device model**	**Electrochemical window (V vs. Li/Li$^+$)**	**Electrode loading**	**Specific capacity**	**Rate capacity**	**Energy density**	**Power density**	**Cyclability**	**Ref.**
Li-SG//SG	Coin cell	0-4.0 V (0.01-4.1V)	Cathode:1-7 mg cm^{-2}	94 F g^{-1} (105mAh g^{-1}) at 0.2 A g^{-1}	30 mAh g^{-1} at 2.0 A g^{-1}	222 Wh kg^{-1} at 410 W kg^{-1}	-	5000 cycles at 0.2 A g^{-1} with a 58% capacity retention	1
Graphite//G@HMMC850	Coin cell	2.0-4.6 V	Cathode: 4 mg Anode: 2 mg	112 mAh g^{-1} at 0.2 A g^{-1}	73.3 mAh g^{-1} at 8.0 A g^{-1}	233.3 Wh kg^{-1} at 450.4 W kg^{-1}	15.7 kW kg^{-1} at 143.8 Wh kg^{-1}	3000 cycles at 1.0 A g^{-1}	2
HOG-Li//AC	Coin cell	1.5-4.2 V	Cathode: 11-13 mg cm^{-2} Anode: 5 mg cm^{-2}	73.1 mAh g^{-1} at 0.02 A g^{-1}	43.1 mAh g^{-1} at 1.0 A g^{-1}	231.7 Wh kg^{-1} at 57 W kg^{-1}	2.8 kW kg^{-1} at 131.9 Wh kg^{-1}	1000 cycles at 0.5 A g^{-1} with a 84.2% capacity retention	3
BNC//BNC	Coin cell	0-4.5 V	1.5-2 mg cm^{-2}	94 F g^{-1} at 0.1 A g^{-1}	94 F g^{-1} at 0.1 A g^{-1}	220 Wh kg^{-1} at 225 W kg^{-1}	22.5 kW kg^{-1} at 104 Wh kg^{-1}	5000 cycles at 2.0 A g^{-1} with a 81% capacity retention	4
GNS//HN-PPs	Coin cell	1.2-4.5 V	~1.0 mg cm^{-2} total electrode weight 2-3 mg cm^{-2}	98 mAh g^{-1} at 0.1 A g^{-1}	-	265 Wh kg^{-1} at 298 W kg^{-1}	5.081 kW kg^{-1} at 210 Wh kg^{-1}	2000 cycles at 1.0 A g^{-1} with a 70% capacity retention	5
Fe_3O_4/G//3DG Graphene	Coin cell	1.0-4.0 V	Cathode: 0.4 g cm^{-3} Anode: 1.5 mg cm^{-2}	-	-	147 Wh kg^{-1} at 150 W kg^{-1}	2.587 kW kg^{-1} at 86 Wh kg^{-1}	1000 cycles at 2.0 A g^{-1} with a 70% capacity retention	6
Si/Cu fabric//AC	Coin cell	1.5-4.2 V	Cathode: 0.2-3 mg cm^{-3}	156 F g^{-1} at	68 F g^{-1} at 20	210 Wh kg^{-1} at	99 kW kg^{-1} at 43	1500 cycles at 5.0 A g^{-1} with a 70%	7

			Anode: 0.5 mg cm^{-2}	0.1 A g^{-1}	A g^{-1}	193 W kg^{-1}	Wh kg^{-1}	capacity retention	
Si/C//RH-AC	Coin cell	2.0-4.0 V	Cathode: 2 mg Anode: 1 mg	144 F g^{-1} at 0.1 A g^{-1}	114 F g^{-1} at 12.8 A g^{-1}	227 Wh kg^{-1} at 1146 W kg^{-1}	32.595 kW kg^{-1} at 181 Wh kg^{-1}	16000 cycles at 6.4 A g^{-1}	8
N-CNPipes//PRGO	Coin cell	0.01-4.0 V	Cathode: 2-2.5 mg Anode: 2-2.5 mg	160 F g^{-1} at 0.45 A g^{-1}	40 F g^{-1} at 9 A g^{-1}	262 Wh kg^{-1} at 450 W kg^{-1}	9.0 kW kg^{-1} at 78 Wh kg^{-1}	4000 cycles at 6.4 A g^{-1} with a 91% capacity retention	9
Li//$LiNi_{0.6}Mn_{0.2}Co_{0.2}O_2$	Pouch cell	2.7-4.4 V	Cathode: 21.4 mg cm^{-2}	-	-	300 Wh kg^{-1} at 450 W kg^{-1}	-	200 cycles at C/10 charge, C/3 discharge with a 86% capacity retention	10
$Li_{22}Sn_5$//$LiFePO_4$	Coin cell	2.5-4.0 V	Cathode: 6.5 mg cm^{-2}	132 mAh g^{-1} at 5C	-	-	-	500 cycles at 5C with a 91% capacity retention	11
q-PET/Li//$Li_4Ti_5O_{12}$	Coin cell	1.0-3.0 V	-	~110 mAh g^{-1} at 2C	-	-	-	1000 cycles at 2C	12
Li-3DAGBN//$LiNi_{0.5}Mn_{0.3}Co_{0.2}O_2$	Coin cell		Cathode: 21.4 mg cm^{-2}	~147 mAh g^{-1} at 10C	~116 mAh g^{-1} at 20C	-	-	1000 cycles at 2C with a ~40% capacity retention	13
Li-Au@CCS//3D-SAC	**Coin cell**	**1.5-4.2 V**	**1.8 mg cm^{-2}(2 mg)**	**230 F g^{-1} at 0.1 A g^{-1}**	**121 F g^{-1} at 10 A g^{-1}**	**492 Wh kg^{-1} at 285 W kg^{-1}**	**28.5 kW kg^{-1} at 259 Wh kg^{-1}**	**2500 cycles at 2A g^{-1} with a 89.3% capacity retention**	**Our work**

Note: The performance values of LICs provided in Table S6 were calculated based on the total mass of both anode and cathode. For LMBs, the values of coin cells were based on the mass of the cathode and the values of pouch cells were calculated based on the total mass of the device.

Table S2 The weight distributions of all the cell components in the cell.

Cell components	Weight (mg)	Percentage
Electrolyte/ 1 M $LiPF_6$ (EC:DEC, v/v=1:1)	3.33	36.47
Separator (Celgard 2400 with a diameter of 14 mm)	2.35	25.74
Current collector (flexible CNT film with a diameter of 12 mm, 0.35x2)	0.7	7.67
Cathode material (3D-SAC)	2.0	21.9
Anode material (electrodeposited Li)	0.25	2.74
Additive (binder and conductive agent)	0.5	5.48
Total	9.13	100

References

[1] Y. G. Sun, J. Tang, F. X. Qin, J. S. Yuan, K. Zhang, J. Li, D. M. Zhu, L. C. Qin, *J. Mater. Chem. A,* **2017**, 5, 13601-13609.

[2] N. W. Li, X. Y. Du, J. L. Shi, X. L. Zhang, W. Fan, J. N. Wang, S. Y. Zhao, Y. B. Liu, W. H. Xu, M. C. Li, Y. G. Guo, C. J. Li, *Electrochim. Acta,* **2018**, 281, 459-465.

[3] W. Ahn, D. U. Lee, G. Li, K. Feng, X. L. Wang, A. P. Yu, G. Lui, Z. W. Chen, *ACS Appl. Mater. Interfaces,* **2016**, 8, 25297-25305.

[4] Q. Y. Xia, H. Yang, M. Wang, M. Yang, Q. B. Guo, L. M. Wan, H. Xia, Y. Yu, *Adv. Energy Mater.,* **2017**, 7, ~~1701336~~9.

[5] N. R. Kim, S. M. Lee, M. W. Kim, H. J. Yoon, W. G. Hong, H. J. Kim, H. J. Choi, H. J. Jin, Y. S. Yun, *Adv. Energy Mater.,* **2017**, 7, ~~7~~1700629.

[6] F. Zhang, T. F. Zhang, X. Yang, L. Zhang, K. Leng, Y. Huang, Y. S. Chen, *Energy Environ. Sci,.* **2013**, 6, 1623-1632.

[7] C. M. Lai, T. L. Kao, H. Y. Tuan, *J. Power Sources,* **2018**, 379, 261-269.

[8] B. Li, Z. J. Xiao, M. Chen, Z. Y. Huang, X. Y. Tie, J. T. Zai, X. F. Qian, *J. Mater. Chem. A,* **2017**, 5, 24502-24507.

[9] D. P. Dubal, P. Gomez-Romero, *Mater. Today Energy,* **2018**, 8, 109-117.

[10] C. J. Niu, H. Lee, S. R. Chen, W. Xu, J. G. Zhang, J. Xiao, J. Liu, *Nat. energy,* **2019**, 4, 551-559.

[11] M. T. Wan, S. J. Kang, L. Wang, H. W. Lee, G. W. Zheng, Y. Cui, Y. M. Sun, *Nat. Commun.,* **2020**, 11, 10.

[12] W. D. Zhang, H. L. L. Zhuang, L. Fan, L. N. Gao, Y. Y. Lu, *Sci. Adv.,* **2018**, 4, 8.

[13] P. Xue, S. R. Liu, X. L. Shi, C. Sun, C. Lai, Y. Zhou, D. Sui, Y. S. Chen. J. J. Liang, *Adv. Mater.,* **2018**, 30, 10.